PHYSICAL REVIEW B **96**, 201304(R) (2017)

Ultracoherent operation of spin qubits with superexchange coupling

Marko J. Rančić* and Guido Burkard†
Department of Physics, University of Konstanz, D-78457 Konstanz, Germany
(Received 10 May 2017; revised manuscript received 9 October 2017; published 7 November 2017)

With the use of nuclear-spin-free materials such as silicon and germanium, spin-based quantum bits (qubits) have evolved to become among the most coherent systems for quantum information processing. The new frontier for spin qubits has therefore shifted to the ubiquitous charge noise and spin-orbit interaction, which are limiting the coherence times and gate fidelities of solid-state qubits. In this paper we investigate superexchange, as a means of indirect exchange interaction between two single electron spin qubits, each embedded in a single semiconductor quantum dot (QD), mediated by an intermediate, empty QD. Our results suggest the existence of "supersweet spots", in which the qubit operations implemented by superexchange interaction are simultaneously first-order-insensitive to charge noise and to errors due to spin-orbit interaction. The proposed spin-qubit architecture is scalable and within the manufacturing capabilities of semiconductor industry.

DOI: 10.1103/PhysRevB.96.201304

Introduction. Noise-insensitive control of qubits is an important task in quantum information science [1–4]. In addition to its use for two-qubit operations of single electron spin qubits [5], the exchange interaction has been utilized to control double [5–8] and triple electron spin qubits [9–12] in semiconductor quantum dots (QDs). However, overcoming the sensitivity of exchange interaction to charge noise [2,3] and errors originating from spin-orbit interaction [13,14] has proved to be a challenging task.

Three electron spin qubits can be operated close to a "sweet spot", where the sensitivity of exchange interaction to charge noise vanishes in first order [10–12,15]. On the other hand, two-electron $S-T_0$ spin qubits embedded in double QDs, only have a trivial first-order sweet spot, where the exchange interaction is smallest ($\sim t^2/U$). A possibility to reduce the sensitivity of the $S-T_0$ qubit to electric noise is to control the magnitude of the exchange interaction by controlling the tunnel coupling instead of controlling the detuning between the two dots (symmetric operation) [16,17].

The spin-orbit interaction represents a powerful resource to control spin qubits [18,19]. On the other hand, it can also reduce the coherence time of the electron spin qubit, hamper efforts to prolong the coherence time of the electron spin qubit [20,21], and lead to errors in two-qubit operations [13,14].

Superexchange is the underlying mechanism responsible for the creation of antiferomagnetic order in CuO and MnO [22,23], is a possible mechanism for d-wave high T_c superconductivity [24], and allows for switching between ferromagnetic and anti-ferromagnetic order in cold atomic gases [25]. Although the possibility to use mediated exchange (superexchange) was mentioned in the original Loss-DiVincenzo proposal [1], superexchange has not received significant attention from the spin qubit community (see, however, Refs. [26–30]). One of the reasons for this lies in the fact that compared to the direct exchange superexchange requires an additional quantum dot.

In this theoretical paper, we investigate superexchange, the exchange interaction between two single electron spin qubits, each embedded in a semiconductor QD on the left (L) and right (R), mediated by an empty quantum dot in the center (C) [see Fig. 1(a)]. We have discovered a parameter regime in which the superexchange is nonzero and is simultaneously insensitive to both charge noise and errors due to spin-orbit interaction in first order (a nontrivial first-order "supersweet spot"). Our further findings suggest that the sign and the magnitude of superexchange can be controlled by varying the detunings between the QDs.

Model. The superexchange is a fourth-order tunneling process, in which the (1,0,1) charge state with antiparallel spins, virtually tunnels via the (1,1,0) or (0,1,1) state to the (2,0,0), (0,2,0) or (0,0,2) charge state, followed by a tunneling back to the (1,1,0) or (0,1,1) state and finally again to the (1,0,1) charge state, but with the spin state of the L and R QD exchanged, as shown in Fig. 1(b).

We describe the system with a generalized Hubbard Hamiltonian $H = H_0 + H'$ for two electrons in a triple quantum dot,

$$H_0 = \sum_{i\sigma} \left(\varepsilon_i + E_z^i \sigma\right) n_{i\sigma} + U \sum_i n_{i\uparrow} n_{i\downarrow} + \sum_{\langle ij\rangle} V n_i n_j, \quad (1)$$

$$H' = \sum_{\langle ij\rangle} \left[\sum_{\sigma} t_{ij} c_{i\sigma}^\dagger c_{j\sigma} + \sum_{\sigma\neq\bar{\sigma}} t_{ij}^{\mathrm{so}} c_{i\sigma}^\dagger c_{j\bar{\sigma}} \right]. \quad (2)$$

Here, E_z is the Zeeman energy due to an external magnetic field, t_{ij} and t_{ij}^{so} are the magnitudes of spin-conserving and spin-orbit-induced spin-non-conserving tunnel hoppings, respectively, between dots i and j. Furthermore, ε_i denotes the energy bias of the ith dot, U is the Coulomb penalization of the doubly occupied quantum dot, V is the Coulomb energy of two neighboring dots occupied with single electrons and $n_i = n_{i\uparrow} + n_{i\downarrow} = c_{i\uparrow}^\dagger c_{i\uparrow} + c_{i\downarrow}^\dagger c_{i\downarrow}$ the number operator, with $c_{i\sigma}(c_{i\sigma}^\dagger)$ being the spin creation (annihilation) operator of the i charge state with spin $\sigma = \downarrow, \uparrow$. The $\langle ij\rangle$ in the index of the sum denotes that the sum runs over nearest neighbor QDs i and j, and the index $\sigma \neq \bar{\sigma}$ denotes a restricted double sum which runs over all possible states of different spin.

*Present address: Department of Physics, University of Basel, Klingelbergstrasse 82, CH-4056 Basel, Switzerland; marko.rancic@unibas.ch
†guido.burkard@uni-konstanz.de

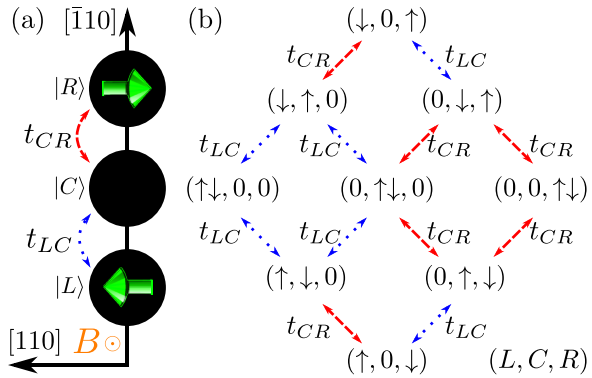

FIG. 1. (a) The geometry of the system, where B denotes the direction of the external magnetic field, t_{LC} are spin-conserving hoppings between the left (L) and center (C) dot (marked with dotted blue lines), t_{CR} are spin-conserving hoppings between the C and the right (R) dot (marked with dashed red lines), and [110] and [$\bar{1}$10] are the crystallographic axes. (b) The scheme of all possible superexchange paths in absence of spin-orbit interactions. All superexchange paths involve four tunneling events, two between the L and the C QDs t_{LC} and two between the C and the R QDs t_{CR}. ↑ stands for a spin-up state, ↓ for a spin-down state and fields in the parentheses denote charge occupancies of the (L,C,R) QDs.

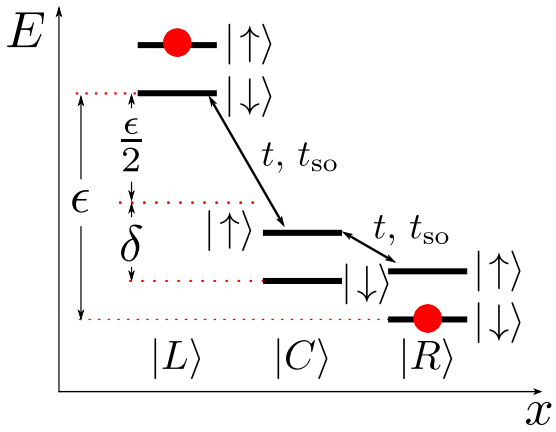

FIG. 2. Level diagram, where E denotes the energy, x the position, ϵ is the energy difference between the outer dots (L and R), and δ the energy between the average energy of the outer dots (L and R) and the center (C) QD.

The Coulomb repulsion of doubly occupied quantum dots is characterized by an energy of $U \sim 1$ meV, and the Coulomb repulsion of neighboring dots being occupied $V \sim 0.1U - 0.01U$. Therefore we neglect the Coulomb repulsion of neighboring dots for simplicity. We also assume a linear triple QD arrangement, allowing us to neglect direct hopping between the R and the L dots, $t_{LR} = t_{LR}^{so} = 0$. Furthermore, from now on, we will assume that $t_{LC} = t_{CR} = t$, $t_{LC}^{so} = t_{CR}^{so} = t_{so}$, a 2DEG in the (001) plane of a zinc-blende semiconductor and Rashba α and Dresselhaus β spin-orbit constants of same signs [31]. This means that the magnitude of the spin-orbit hopping t_{so} is maximal when the linear triple quantum dot is structured along the [$\bar{1}$10] crystallographic axis and minimal when the triple quantum dot is structured along [110] [see Fig. 1(a)]. The relation between the spin-conserving t and spin-non-conserving t_{so} hopping is given by $t_{so} = 4tl/(3\Lambda_{so})$, where l is the interdot separation, and $\Lambda_{so} = \hbar/(m^*\sqrt{(\alpha+\beta)^2\sin^2\phi + (\alpha-\beta)^2\cos^2\phi})$ is the spin-orbit length, where ϕ is the angle between the [110] crystallographic axis and the interdot connection axis. Detunings in the Hamiltonian Eq. (1) can be expressed in terms of two parameters, the detuning between the outer dots ϵ and the detuning between the center dot and average detuning of the outer dots δ, see Fig. 2.

Results. We transform the initial generalized Hubbard Hamiltonian $H = H_0 + H'$ [see Eqs. (1) and (2)] by means of a fourth-order Schrieffer-Wolff (SW) transformation [32–34], yielding an effective Hamiltonian in which the superexchange subspace $s = \{(\uparrow,0,\downarrow), (\downarrow,0,\uparrow), (\uparrow,0,\uparrow), (\downarrow,0,\downarrow)\}$ is decoupled from the 11 dimensional subspace of high energy states $h = \{(\uparrow,\downarrow,0), (\downarrow,\uparrow,0), (\uparrow,\uparrow,0), (\downarrow,\downarrow,0), (0,\uparrow,\downarrow), (0,\downarrow,\uparrow), (0,\uparrow,\uparrow), (0,\downarrow,\downarrow), (\uparrow\downarrow,0,0), (0,\uparrow\downarrow,0), (0,0,\uparrow\downarrow)\}$ (see Ref. [35] at for more details about the SW transformation). For a linear quantum dot structured along [$\bar{1}$10] and an external magnetic field parallel to the (001) direction, the effective Hamiltonian up to forth order in perturbation theory in t_{ij} and t_{ij}^{so} within the superexchange subspace s is

$$\tilde{H} = J_{SE}\mathbf{S}_L \cdot \mathbf{S}_R + D\left(S_L^x - S_R^x\right) + \sum_{i=L,R} E_z^i S_i^z. \quad (3)$$

Here, $\mathbf{S}_L$ and $\mathbf{S}_R$ are spin operators belonging to the L and R QDs and J_{SE} is the magnitude of superexchange involving spin-conserving tunnel hoppings

$$J_{SE} = 4t^4 U \frac{U(12\delta^2+\epsilon^2) - \delta(8\delta^2+6\epsilon^2)}{(\epsilon^2-4\delta^2)^2(U-2\delta)(U^2-\epsilon^2)}. \quad (4)$$

The second term in Eq. (3) is the lowest-order spin-orbit contribution to the exchange coupling, with S_L^x and S_R^x being the x components of the spin operator corresponding to the L and R QD, respectively. The magnitude of the spin-orbit contribution D is given by

$$D = \frac{2E_z t t_{so}\left(4E_z^2 - 4\delta^2 - \epsilon^2\right)}{16\left(E_z^2-\delta^2\right)^2 - 8\left(E_z^2+\delta^2\right)\epsilon^2 + \epsilon^4}. \quad (5)$$

The third term in Eq. (3) is the Zeeman energy with S_i^z being the z component of the spin operator corresponding to $i = L, R$ QD. In the process of deriving Eqs. (3)–(5), we have neglected all terms with a power higher than t^4, and only kept the lowest order contribution involving spin-orbit interaction $\sim t t_{so}$.

A nontrivial superexchange sweet spot is a point in which the superexchange is in first order insensitive to fluctuations of the detuning parameters δ and ϵ, and furthermore the superexchange is not zero. Solving the coupled systems of equations $\partial J_{SE}/\partial\epsilon = 0, \partial J_{SE}/\partial\delta = 0$ and $J_{SE} \neq 0$ for ϵ and δ, in the case of vanishing spin-orbit interaction, we obtain four solutions for ϵ and δ $\epsilon_{1,2} = 0$, $\delta_{1,2} = (5 \pm \sqrt{13})/4$, $\epsilon_{3,4} = \pm 0.745$, $\delta_{3,4} = 0.074$ in units of U and sweet spots $J_1(\delta_1,\epsilon_1) = 0.08$, $J_2(\delta_2,\epsilon_2) = 64.65$, $J_3(\delta_3,\epsilon_3) = J_4(\delta_4,\epsilon_4) = 13.8$ in units of t^4/U^3, where t is the tunneling and U is Coulomb repulsion Fig. 3.

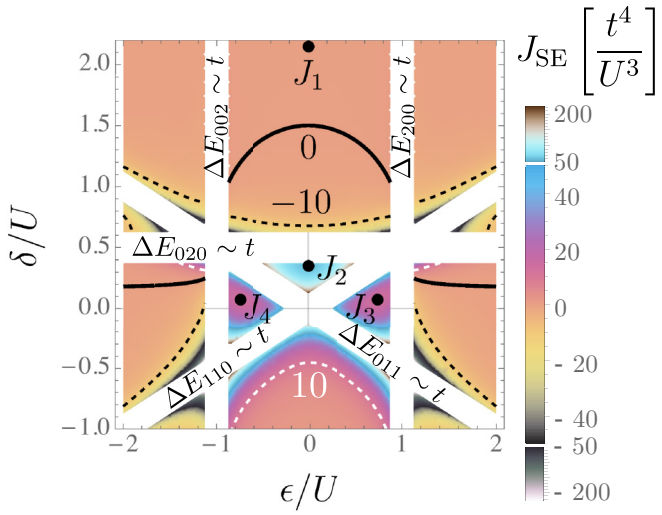

FIG. 3. The superexchange in the absence of spin-orbit interaction $J_{\rm SE}$ as a function of the detuning parameters δ and ϵ. The points represent the superexchange sweet spots $J_1(\delta_1,\epsilon_1) = 0.08$, $J_2(\delta_2,\epsilon_2) = 64.65$, and $J_3(\delta_3,\epsilon_3) = J_4(\delta_4,\epsilon_4) = 13.62$ in units of t^4/U^3, where t is the tunneling and U is Coulomb repulsion. The black line marks $J_{\rm SE} = 0$, black dashed line $J_{\rm SE} = -10$ and white dashed line $J_{\rm SE} = 10$. The white regions represent areas in which the energy difference ΔE between the (2,0,0) (0,2,0) (0,0,2) (1,1,0) (0,1,1) charge states and superexchange states (101) becomes comparable to t, and therefore no superexchange takes place. Here, we chose $t = 17.8\,\mu$eV.

In contrast to a double QD loaded with two electrons, a linear triple QD loaded with two electrons has four points in the parameter space of ϵ and δ in which the exchange interaction is simultaneously first-order insensitive in fluctuation of this two parameters. We also note that that the sweet spots J_2, J_3, and J_4 lie close to the areas in which no superexchange takes place due to leakage outside the superexchange subspace (white regions in Fig. 3). The width of the white areas in Fig. 3 is proportional to tunneling t, and this imposes a limit beyond which the magnitude of superexchange cannot be increased by increasing the tunnel coupling, while simultaneously performing superexchange at the double sweet spot. It should be noted that we can turn superexchange interaction on and off by controlling only the detuning parameters ϵ and δ, so no control of the tunneling parameters t would be needed. This means that our triple quantum dot qubit can be made without additional tunneling gates which would control t. This protects the tunneling hopping t from electric noise induced in the tunneling gate. Furthermore, (super)exchange is robust against variations in the hyperfine magnetic field due to the fact that the speed of the superexchange gate around the sweet spots J_2, J_3, $J_4 \sim 0.2$ ns is much larger then the nuclear spin coherence time in InGaAs ~ 10 ns.

We want to find values of the Zeeman energy E_z for which $D = 0$ around the sweet spots. This would give rise to superexchange simultaneously insensitive to charge noise and spin-orbit effects in first order. By inserting δ_i and ϵ_i ($i = 1, 4$) into Eq. (5), we found that such nonzero values exist corresponding to $\delta_{3,4}$ and $\epsilon_{3,4}$ and therefore to sweet spots $J_{3,4}$, while no nonzero E_z for $\delta_{1,2}$ and $\epsilon_{1,2}$ exists. Two such values of the Zeeman energy exist $E_z^{3,4}/U = \pm 0.38$ for each of the sweet spots J_3 and J_4. The Coulomb repulsion $U \sim 1$ eV in InGaAs quantum dots. The Zeeman energy of $\pm 0.38U$ corresponds to an external magnetic field of $B_{\rm GaAs} = \pm U/0.44\mu_B = \pm 14.9$ T. However, due to a much higher g factor, this field is $B_{\rm InAs} = \pm U/14.7\mu_B = \pm 0.45$ T for InAs, and thus easier to achieve. As shown in Fig. 4(a), the point J_3 at $E_z = \pm 0.38U$ is a supersweet spot in which the superexchange is simultaneously insensitive to charge noise and spin-orbit effects are vanishing. It should be noted that spin-orbit interaction is much stronger in InAs compared to GaAs.

Solving $J_{SE} = 0$ [Eq. (4)], we calculate δ_0 for which the spin-conserving superexchange is zero for any value of ϵ and ϵ_0 for which the superexchange is zero for any value of δ (see Fig. 3),

$$\delta_0 = \frac{1}{2}\left(1 + \frac{1-\epsilon^2}{q^{1/3}} + q^{1/3}\right); \quad \epsilon_0 = \pm\frac{2\sqrt{(3-2\delta)\delta^2}}{\sqrt{6\delta-1}}, \quad (6)$$

where $q = 1 - \epsilon^2 + \sqrt{(\epsilon^2(\epsilon^2-1)^2)}$ all given in units of Coulomb repulsion U. It should be noted that the result is symmetric with respect to the sign of ϵ. When $\epsilon = -1.34U$, at large negative values of the bias δ, the main contribution of the superexchange comes from path 6, which gives rise to negative superexchange (see Table I) as the bias is increased

TABLE I. Six possible superexchange paths involving spin-conserving tunneling with corresponding expressions $J_{\rm SE} = \sum_i J^i_{\rm SE}$. The parameters for which the sign of $J_{\rm SE}$ is valid are the Coulomb repulsion $U = 1$ meV, the detuning between the outer dots $\epsilon = -1.34U$, the detuning between the middle dot and the average of the outer dots $-0.2U < \delta < 0.3U$.

i	Superexchange path	Superexchange expression	Sign of $J^i_{\rm SE}$
1	$(\uparrow,0,\downarrow) \overset{t_{CR}}{\leftrightarrows} (\uparrow,\downarrow,0) \overset{t_{LC}}{\leftrightarrows} (0,\uparrow\downarrow,0) \overset{t_{LC}}{\leftrightarrows} (\downarrow,\uparrow,0) \overset{t_{CR}}{\leftrightarrows} (\downarrow,0,\uparrow)$	$t^4/[(U-2\delta)(\epsilon/2+\delta)^2]$	$J^1_{\rm SE} > 0$
2	$(\uparrow,0,\downarrow) \overset{t_{LC}}{\leftrightarrows} (0,\uparrow,\downarrow) \overset{t_{CR}}{\leftrightarrows} (0,\uparrow\downarrow,0) \overset{t_{CR}}{\leftrightarrows} (0,\downarrow,\uparrow) \overset{t_{LC}}{\leftrightarrows} (\downarrow,0,\uparrow)$	$t^4/[(U-2\delta)(\epsilon/2-\delta)^2]$	$J^2_{\rm SE} > 0$
3	$(\uparrow,0,\downarrow) \overset{t_{CR}}{\leftrightarrows} (\uparrow,\downarrow,0) \overset{t_{LC}}{\leftrightarrows} (0,\uparrow\downarrow,0) \overset{t_{CR}}{\leftrightarrows} (0,\downarrow,\uparrow) \overset{t_{LC}}{\leftrightarrows} (\downarrow,0,\uparrow)$	$-t^4/[(U-2\delta)(\epsilon/2-\delta)(\epsilon/2+\delta)]$	$J^3_{\rm SE} < 0$
4	$(\uparrow,0,\downarrow) \overset{t_{LC}}{\leftrightarrows} (0,\uparrow,\downarrow) \overset{t_{CR}}{\leftrightarrows} (0,\uparrow\downarrow,0) \overset{t_{LC}}{\leftrightarrows} (\downarrow,\uparrow,0) \overset{t_{CR}}{\leftrightarrows} (\downarrow,0,\uparrow)$	$-t^4/[(U-2\delta)(\epsilon/2-\delta)(\epsilon/2+\delta)]$	$J^4_{\rm SE} < 0$
5	$(\uparrow,0,\downarrow) \overset{t_{CR}}{\leftrightarrows} (\uparrow,\downarrow,0) \overset{t_{LC}}{\leftrightarrows} (\uparrow\downarrow,0,0) \overset{t_{LC}}{\leftrightarrows} (\downarrow,\uparrow,0) \overset{t_{CR}}{\leftrightarrows} (\downarrow,0,\uparrow)$	$t^4/[(U-\epsilon)(\epsilon/2+\delta)^2]$	$J^5_{\rm SE} > 0$
6	$(\uparrow,0,\downarrow) \overset{t_{LC}}{\leftrightarrows} (0,\uparrow,\downarrow) \overset{t_{CR}}{\leftrightarrows} (0,0,\uparrow\downarrow) \overset{t_{CR}}{\leftrightarrows} (0,\downarrow,\uparrow) \overset{t_{LC}}{\leftrightarrows} (\downarrow,0,\uparrow)$	$t^4/[(U+\epsilon)(\epsilon/2-\delta)^2]$	$J^6_{\rm SE} < 0$

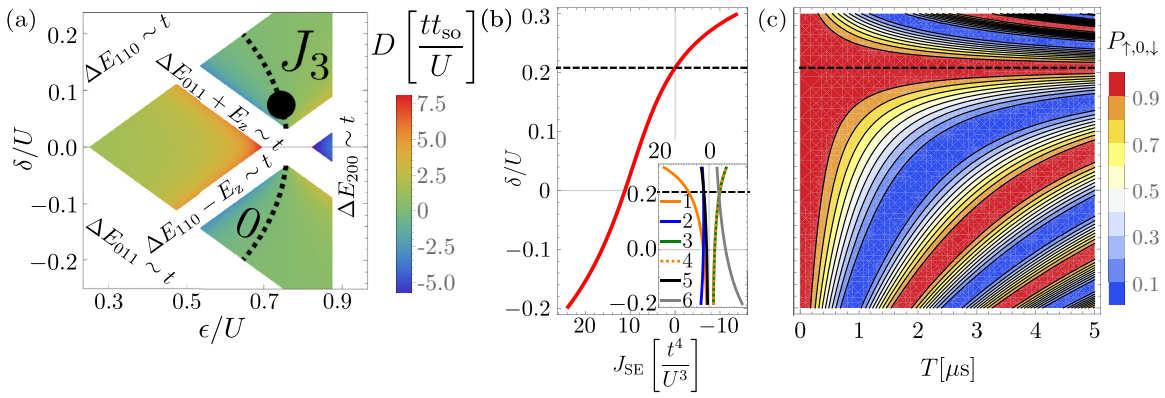

FIG. 4. (a) The strength of the spin-orbit contribution D around the "sweet spot" J_3 as a function of the detuning parameter ϵ and δ for $E_z = 0.38U$. The dashed black line marks a path along which $D = 0$. (b) Superexchange as a function of δ for $\epsilon = -1.34$ U in the case of vanishing spin orbit. (Inset) Magnitude of different exchange paths in the context of Table I in the case of vanishing spin orbit. The horizontal black dashed line represents the point δ_0 in which $J_{SE} = 0$. (c) Coherent superexchange oscillations as a function of the detuning δ and time T in the case of vanishing spin-orbit interaction. The probability to occupy the $(\downarrow,0,\uparrow)$ state is not displayed because $P_{\uparrow 0\downarrow} = 1 - P_{\downarrow 0\uparrow}$. Parameters of the plots are tunneling $t = 17.8\,\mu$eV, detuning $\epsilon = -1.34$ U, the Coulomb repulsion $U = 1$ meV.

towards the positive values, the superexchange path 1 becomes more dominant yielding a positive sign of superexchange [see Figs. 4(b) and 4(b), inset].

Now we will investigate the dynamical evolution of spin states caused by superexchange interaction in the absence of spin-orbit interaction. We start by initializing a $(\uparrow,0,\downarrow)$ state. The time evolution of the system in the superexchange subspace is modeled in the following way: $\psi_{SE}(T) = \mathcal{U}\psi_{SE}(0)$, where $\psi_{SE}(0)$ is the initial wave function corresponding to the initialization of the $(\uparrow,0,\downarrow)$ state, $\psi_{SE}(T)$ the wave function at time T, and $\mathcal{U} = \exp(-i\tilde{H}T/\hbar)$ where $\tilde{H}$ is given by Eq. (3). In Fig. 4(d), we observe that superexchange oscillations are suppressed around the point $\delta = \delta_0$. Areas above and below the black line correspond to different signs of superexchange.

Conclusion. We have investigated coherent superexchange and found points in parameter space in which the superexchange is both insensitive to charge noise and the spin-orbit contribution is zero. Furthermore, we have shown that the sign of the superexchange can be changed by varying the detuning parameters. An experimental implementation of our findings would allow for charge noise-insensitive, error-free two-qubit operation of the spin 1/2 qubit and charge-noise-insensitive, error-free control of the $S - T_0$ qubit around the exchange axis. The implications of our findings to the operation of the exchange only qubit in a charge-noise-insensitive manner are planned as a forthcoming investigation.

Acknowledgments. We acknowledge funding from the EU within the Marie Curie ITN Spin-Nano and the German Research Foundation within the SFB 767.

[1] D. Loss and D. P. DiVincenzo, Phys. Rev. A **57**, 120 (1998).
[2] G. Burkard, D. Loss, and D. P. DiVincenzo, Phys. Rev. B **59**, 2070 (1999).
[3] X. Hu and S. Das Sarma, Phys. Rev. Lett. **96**, 100501 (2006).
[4] R. Hanson, L. P. Kouwenhoven, J. R. Petta, S. Tarucha, and L. M. K. Vandersypen, Rev. Mod. Phys. **79**, 1217 (2007).
[5] J. R. Petta, A. C. Johnson, J. M. Taylor, E. A. Laird, A. Yacoby, M. D. Lukin, C. M. Marcus, M. P. Hanson, and A. C. Gossard, Science **309**, 2180 (2005).
[6] J. Levy, Phys. Rev. Lett. **89**, 147902 (2002).
[7] D. Reilly, J. Taylor, J. Petta, C. Marcus, M. Hanson, and A. Gossard, Science **321**, 817 (2008).
[8] X. Wu, D. R. Ward, J. Prance, D. Kim, J. K. Gamble, R. Mohr, Z. Shi, D. Savage, M. Lagally, M. Friesen *et al.*, Proc. Natl. Acad. Sci. USA **111**, 11938 (2014).
[9] D. P. DiVincenzo, D. Bacon, J. Kempe, G. Burkard, and K. B. Whaley, Nature (London) **408**, 339 (2000).
[10] J. Medford, J. Beil, J. Taylor, S. Bartlett, A. Doherty, E. Rashba, D. DiVincenzo, H. Lu, A. Gossard, and C. M. Marcus, Nat. Nanotechnol. **8**, 654 (2013).
[11] J. Medford, J. Beil, J. M. Taylor, E. I. Rashba, H. Lu, A. C. Gossard, and C. M. Marcus, Phys. Rev. Lett. **111**, 050501 (2013).
[12] J. M. Taylor, V. Srinivasa, and J. Medford, Phys. Rev. Lett. **111**, 050502 (2013).
[13] N. E. Bonesteel, D. Stepanenko, and D. P. DiVincenzo, Phys. Rev. Lett. **87**, 207901 (2001).
[14] G. Burkard and D. Loss, Phys. Rev. Lett. **88**, 047903 (2002).
[15] M. Russ and G. Burkard, Phys. Rev. B **91**, 235411 (2015).
[16] M. D. Reed, B. M. Maune, R. W. Andrews, M. G. Borselli, K. Eng, M. P. Jura, A. A. Kiselev, T. D. Ladd, S. T. Merkel, I. Milosavljevic *et al.*, Phys. Rev. Lett. **116**, 110402 (2016).
[17] F. Martins, F. K. Malinowski, P. D. Nissen, E. Barnes, S. Fallahi, G. C. Gardner, M. J. Manfra, C. M. Marcus, and F. Kuemmeth, Phys. Rev. Lett. **116**, 116801 (2016).
[18] S. Nadj-Perge, S. Frolov, E. Bakkers, and L. P. Kouwenhoven, Nature (London) **468**, 1084 (2010).
[19] S. Nadj-Perge, V. S. Pribiag, J. W. G. van den Berg, K. Zuo, S. R. Plissard, E. P. A. M. Bakkers, S. M. Frolov, and L. P. Kouwenhoven, Phys. Rev. Lett. **108**, 166801 (2012).

[20] M. J. Rančić and G. Burkard, Phys. Rev. B **90**, 245305 (2014).
[21] J. M. Nichol, S. P. Harvey, M. D. Shulman, A. Pal, V. Umansky, E. I. Rashba, B. I. Halperin, and A. Yacoby, Nat. Commun. **6**, 7682 (2015).
[22] H. Kramers, Physica **1**, 182 (1934).
[23] P. W. Anderson, Phys. Rev. **79**, 350 (1950).
[24] G. Kotliar and J. Liu, Phys. Rev. B **38**, 5142(R) (1988).
[25] S. Trotzky, P. Cheinet, S. Fölling, M. Feld, U. Schnorrberger, A. M. Rey, A. Polkovnikov, E. Demler, M. Lukin, and I. Bloch, Science **319**, 295 (2008).
[26] M. Trif, F. Troiani, D. Stepanenko, and D. Loss, Phys. Rev. Lett. **101**, 217201 (2008).
[27] R. Sánchez, F. Gallego-Marcos, and G. Platero, Phys. Rev. B **89**, 161402(R) (2014).
[28] T. Baart, T. Fujita, C. Reichl, W. Wegscheider, and L. Vandersypen, Nat. Nanotechnol. **12**, 26 (2016).
[29] C.-Y. Hsieh, Y.-P. Shim, M. Korkusinski, and P. Hawrylak, Rep. Prog. Phys. **75**, 114501 (2012).
[30] Y. X. Cheng, Y. D. Wang, J. H. Wei, Z. G. Zhu, and Y. J. Yan, Phys. Rev. B **95**, 155417 (2017).
[31] S. Giglberger, L. E. Golub, V. V. Bel'kov, S. N. Danilov, D. Schuh, C. Gerl, F. Rohlfing, J. Stahl, W. Wegscheider, D. Weiss *et al.*, Phys. Rev. B **75**, 035327 (2007).
[32] R. Winkler, S. Papadakis, E. De Poortere, and M. Shayegan, *Spin-Orbit Coupling in Two-Dimensional Electron and Hole Systems* (Springer, Berlin, Heidelberg, 2003).
[33] S. Bravyi, D. P. DiVincenzo, and D. Loss, Ann. Phys. **326**, 2793 (2011).
[34] J. Romhányi, G. Burkard, and A. Pályi, Phys. Rev. B **92**, 054422 (2015).
[35] See Supplemental Material at http://link.aps.org/supplemental/10.1103/PhysRevB.96.201304 for more details about the SW transformation.